Influence of Pore Size on the van der Waals Interaction Power Laws in Two-Dimensional Molecules and Materials

Yan Yang,[1] Ka Un Lao,[1] and Robert A. DiStasio Jr.[1,*]

[1] *Department of Chemistry and Chemical Biology, Cornell University, Ithaca, NY 14853 USA*

(Dated: September 5, 2018)

Despite the importance of porous two-dimensional (2D) molecules and materials in advanced technological applications, the question of how void space in these systems alters the van der Waals (vdW) scaling landscape has been largely unanswered. Analytical and numerical models presented herein demonstrate that the mere presence of a pore leads to markedly different vdW scaling across non-asymptotic distances, with certain relative pore sizes yielding power laws ranging from simple monotonic decay to the formation of minima, extended plateaus, and even maxima. These models are in remarkable agreement with first-principles approaches for the 2D building blocks of covalent organic frameworks (COFs), and reveal that COF macrocycles are characterized by power laws with extended plateaus spanning 1−4 nm, while COF bilayers have vdW decay rates that are quite distinct from their non-porous analogs. These unique power laws extend across a range of distances relevant to the nanoscale, and represent a hitherto unexplored avenue towards governing the self-assembly of complex nanostructures from porous 2D molecules and materials.

Two-dimensional (2D) materials like graphene, hexagonal boron nitride, and transition metal dichalcogenides have been under intense research for the past decade due to their favorable electronic, optical, thermal, mechanical, and even biological properties [1–5]. Allowing for variable pore sizes beyond the atomic dimensions in graphene, porous 2D materials such as covalent organic frameworks (COFs) [6–12], metal organic frameworks [13, 14], and porous coordination polymers [15, 16] are endowed with additional properties like permanent porosities, high aspect ratios, and large internal surface areas. As such, 2D materials have enabled the development of numerous technological applications, including (opto-)electronics [17], (photo-)thermal devices [18], energy storage materials [19], (bio-)chemical sensors and filters [19, 20], size-selective catalysts [21], and even drug delivery vectors [22, 23].

The assembly of 2D materials into sophisticated single-layer heterostructures [24] and/or multi-layered architectures (including van der Waals (vdW) heterostructures [25–28]), provides access to even more diverse functionalities, targeted properties, and applications. While the monolayers in 2D materials are mostly formed *via* strong covalent bonds, vdW (dispersion) interactions are the predominant forces between the layers. In fact, these ubiquitous forces are largely responsible for self-assembly, and play a crucial role in determining the structure, stability, and function of systems throughout chemistry, physics, and materials science [29–32]. Arising from non-local electrodynamic correlations between instantaneous charge fluctuations in matter, vdW interactions are quantum mechanical in nature with an influence that spans distances (D) ranging from atomic dimensions (*i.e.*, a few Å) to well beyond the nanoscale [33–35]. At these distances, dimensionality, local response properties, and topology—such as the presence of a pore—can strongly influence the strength and scaling of these fundamental forces [36, 37], and hence the observed system properties.

In this regard, analytic vdW scaling laws (such as D^{-5} or D^{-4} for two parallel insulating wires or plates) only apply to infinite-size systems at asymptotic distances, while rather unusual power laws have been observed in both finite and extended systems at intermediate distances relevant to the nanoscale [37–45]. For example, Gould *et al.* [38] argued that the binding energy of graphite varies as D^{-4} for non-asymptotic interlayer separations, which differs from the asymptotic D^{-3} behavior analytically demonstrated by Dobson and co-workers [38, 46, 47]; this was later confirmed by quantum Monte Carlo [39] and the random phase approximation [41], which found $D^{-4.2}$ for $D \approx 3{-}9$ Å. For C_{60} interacting with graphene and a carbon nanotube, Dappe *et al.* [40] observed D^{-3} and $D^{-3.5}$ scaling behavior, respectively, at distances shorter than the C_{60} diameter, in stark contrast to their D^{-4} and D^{-5} asymptotes. Topologically speaking, this example demonstrates that the void space present in these systems has a profound influence over the vdW scaling laws, and governs the (relative) length scales over which one observes deviations from asymptotic behavior. Since even slight variations in these power laws can markedly impact properties and functionalities, such unusual intermediate-range scaling behavior demands further theoretical investigation.

Despite the importance of porous 2D building blocks in the discovery and development of advanced materials, the question of how void space—provided here by variable pore sizes ranging from a few Å to 10s of nm—affects the vdW interaction strength and scaling has been less studied. In this Letter, we present a series of analytical and numerical results that demonstrate how variable pore sizes fundamentally alter the vdW scaling landscape in

* distasio@cornell.edu

three prototypical model systems representing an atom and a porous macrocycle, a porous macrocycle dimer, and a porous periodic bilayer. In doing so, we find that certain pore sizes lead to rather unexpected behavior at short and intermediate distances, and the degree and extent to which these deviations differ from asymptotic behavior can be tuned by varying the relative size and shape of these void spaces. We then show that these simple models are in remarkable agreement with first-principles based vdW methods for a number of popular COF building blocks, and find that such systems are characterized by power laws exhibiting extended plateaus that span 1−4 nm—a range of distances quite relevant to the self-assembly of complex COF architectures [48, 49].

Throughout this work, we quantify the scaling of the vdW interaction energy, $E_{\rm vdW}$, between two objects separated by a distance, D_{AB}, through the effective power law exponent, $P_{\rm vdW}(D)$, defined as [37]:

$$P_{\rm vdW}(D) = \left(\frac{\partial \ln |E_{\rm vdW}(D_{AB})|}{\partial \ln D_{AB}} \right) \Bigg|_{D_{AB}=D}. \qquad (1)$$

As such, $P_{\rm vdW}(D)$ provides an effective measure of the $E_{\rm vdW}(D)$ decay rate and delineates the length scales over which the system deviates from asymptotic behavior.

We begin by considering a point particle, A, separated by D from the center of an annulus with inner and outer radii, r and R, as a model for the interaction of an atom with a porous macrocycle (Fig. 1). To investigate the vdW scaling behavior in this prototypical model system, we analytically derive $P_{\rm vdW}$ based on a second-order perturbative (pairwise) treatment of $E_{\rm vdW}$ and compare our findings to an infinite-order many-body expansion of $E_{\rm vdW}$ *via* the adiabatic-connection fluctuation-dissipation theorem (ACFDT). Assuming that the annulus (denoted by ann$[r, R]$) is continuous and insulating, comprised of a single atom type, and located outside of density overlap with A, the pairwise $E_{\rm vdW} = -\sum_B C_6^{AB} R_{AB}^{-6}$ can be computed by integrating over all annulus surface elements, $\mathrm{d}\sigma_B$, located at a distance, R_{AB}, from A, *i.e.*,

$$E_{\rm vdW}^{A-{\rm ann}}(r, R, D) = -\frac{C_6^{AB}}{S_B} \int \mathrm{d}\sigma_B \, R_{AB}^{-6}, \qquad (2)$$

wherein $S_B = \int \mathrm{d}\sigma_B$ is the annulus surface area. This integral can be analytically evaluated using cylindrical coordinates to yield $P_{\rm vdW}^{A-{\rm ann}}(r, R, D) = -4/[1+(r/D)^2] - 4/[1+(R/D)^2] + 4/[2+(r/D)^2+(R/D)^2]$, which is plotted as a function of r and D for ann$[r, R = 10$ Å$]$ in Fig. 1.

For $r = 0$, the annulus becomes a closed (non-porous) disk and $P_{\rm vdW}^{A-{\rm disk}}(R, D) = P_{\rm vdW}^{A-{\rm ann}}(0, R, D) = -4 - 4/[1+(R/D)^2] + 4/[2+(R/D)^2]$. In the short range, $R/D \to \infty$ and this finite-sized disk mimics an infinite plate from the perspective of A; in this case, one analytically recovers the expected result of $P_{\rm vdW}^{A-{\rm disk}} = -4$ for an atom interacting with an extended (2D) surface [50, 51]. This

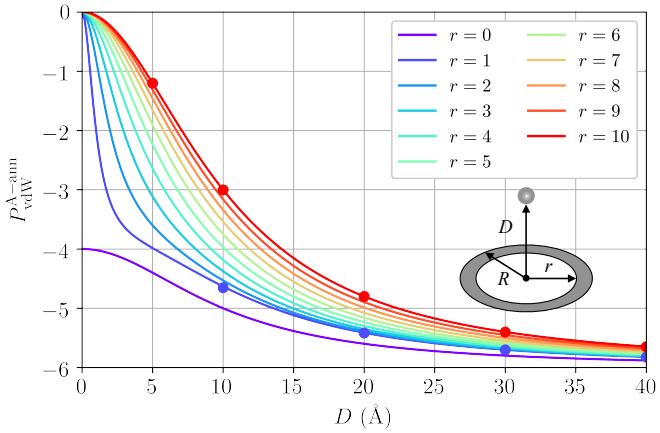

FIG. 1. Effective power law exponents, $P_{\rm vdW}^{A-{\rm ann}}$, for the pairwise (lines) and many-body (circles) vdW interaction between a point particle and an annulus with $R = 10$ as a function of r and D (all in Å). The mere presence of a pore fundamentally alters the vdW scaling landscape and leads to a markedly slower $E_{\rm vdW}^{A-{\rm ann}}$ decay rate across all non-asymptotic distances.

is followed by monotonic decay with D as $R/D \to 0$ and $P_{\rm vdW}^{A-{\rm disk}} \to -6$, which is consistent with the well-known asymptotic expression for two finite-sized systems obtained from non-relativistic quantum mechanics (*i.e.*, $E_{\rm vdW} \propto D^{-6}$). From this figure, one immediately sees that the mere presence of a pore fundamentally alters the vdW scaling landscape across all non-asymptotic distances. In the short range, we find that $P_{\rm vdW} \to 0$ when $r \neq 0$, as the transverse force on A originating from the vdW interaction with the porous annulus vanishes. The presence of a pore also leads to a markedly slower $E_{\rm vdW}$ decay rate across a wide range (0−40 Å) of distances, with $P_{\rm vdW}$ finally approaching (to $\approx 1\%$) the asymptotic limit of -6 for $D \gtrsim 70$ Å. Bound by the limiting cases of $r = 0$ (closed disk) and $r \to R$ (infinitely-thin ring, with $P_{\rm vdW}^{A-{\rm ring}}(R, D) = P_{\rm vdW}^{A-{\rm ann}}(R, R, D) = -6/[1 + (R/D)^2]$), variations in the relative pore size (r/R) and R can be used to tune the extent and length scales over which the system deviates from asymptotic behavior.

Since the inclusion of many-body vdW interactions often lead to power laws with significant deviations from conventional pairwise predictions [37, 43, 51–54], we now consider how an infinite-order many-body expansion of $E_{\rm vdW}^{A-{\rm ann}}$ would influence the vdW scaling behavior in the presence of a pore. Under the same assumptions as above, we computed $P_{\rm vdW}^{A-{\rm ann}}$ for the smallest ($r = 1$ Å) and largest ($r = R = 10$ Å) pore sizes within the random phase approximation (RPA) of the ACFDT (see Supplemental Material) [55]. This approach provides an accurate description of the vdW interaction by accounting for collective many-body effects and electrodynamic response screening in the long-range correlation energy [56–59]. Our ACFDT-RPA results [55] are plotted in Fig. 1 and are in remarkable agreement with $P_{\rm vdW}^{A-{\rm ann}}$, thereby

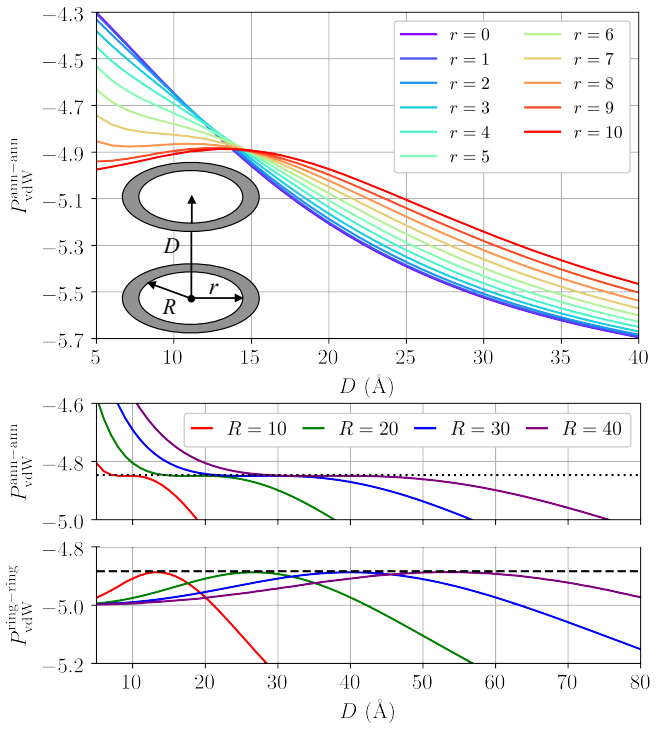

FIG. 2. *Top.* Effective power law exponents, $P_{\rm vdW}^{\rm ann-ann}$, for the pairwise vdW interaction between two stacked annuli with $R = 10$ as a function of r and D (all in Å). Depending on the relative pore size, $P_{\rm vdW}$ exhibits widely varying behavior at non-asymptotic distances, ranging from simple monotonic decay (closed disks) to extended plateaus and maxima (rings). *Bottom.* Extended plateaus (shown here for $R = 10$–40 Å) occur for annuli with $r/R = 0.75$ at $P_{\rm vdW} = -4.85$ (dotted line), and coincide with the stationary point of inflection. Maxima of $P_{\rm vdW} = -4.88$ (dashed line) occur for rings at a relative distance of $D/R = 1.33$.

validating our pairwise treatment of this model system. We attribute this to the fact that the void space hinders delocalization of the polarizability across the annulus, and therefore suppresses the influence of many-body effects in $P_{\rm vdW}^{A-{\rm ann}}$.

Next we consider two annuli in a sandwich configuration as a model system for two stacked porous macrocycles (Fig. 2). Under the same assumptions as above, the pairwise $E_{\rm vdW} = -\sum_{AB} C_6^{AB} R_{AB}^{-6}$ was computed by integrating over the surface elements, $\mathrm{d}\sigma_A$ and $\mathrm{d}\sigma_B$, located on each annulus, *i.e.*,

$$E_{\rm vdW}^{\rm ann-ann}(r,R,D) = -\frac{C_6^{AB}}{S_A S_B}\int \mathrm{d}\sigma_A \int \mathrm{d}\sigma_B\, R_{AB}^{-6}. \quad (3)$$

This integral can also be evaluated analytically in a cylindrical coordinate system to obtain $P_{\rm vdW}^{\rm ann-ann}(r,R,D)$, which is plotted in the top panel of Fig. 2 for two annuli with $R = 10$ Å, and whose general form is given in Ref. [55]. From this figure, one again sees that the presence of a pore leads to non-trivial changes in $P_{\rm vdW}$ across non-asymptotic D; depending on r/R, $P_{\rm vdW}$ exhibits widely varying behavior, ranging from simple monotonic decay to the formation of extended plateaus and maxima.

In the absence of a pore, $P_{\rm vdW}^{\rm disk-disk}(R,D) = -4 - 2/[1+(R/D)^2]$ has a monotonically decaying form which analytically yields the expected limits of D^{-4} and D^{-6} for short and asymptotic D (*vide supra*). As r increases, radically different behavior emerges with the formation of extended plateaus in $P_{\rm vdW}$. Mathematically speaking, such an extended plateau in $P_{\rm vdW}$ corresponds to a stationary point of inflection, wherein both $\partial P_{\rm vdW}/\partial D$ and $\partial^2 P_{\rm vdW}/\partial D^2$ vanish. These conditions form an underdetermined set of equations that can be analytically solved [55] to yield the relative pore size, $r/R = 0.75$, and distance, $D/R = 0.91$, corresponding to this inflection point. As depicted in the bottom panel of Fig. 2 for two ann$[0.75R, R]$ with $R = 10$–40 Å, these plateaus have an analytical value of $P_{\rm vdW} = -4.85$, and this enhanced vdW interaction spans a remarkably wide distance range. To approximate the spatial extent of these plateaus, we located the values of D when $P_{\rm vdW} = -4.85 \pm 0.05$ (a range equivalent to the dotted line width) and determined that this enhancement persists for $D = 0.45R$–$0.55R$. In what follows, we will show that several popular COF macrocycles have $r/R \approx 0.75$, and hence their $P_{\rm vdW}$ exhibit extended plateaus across a range of distances quite relevant to self-assembly.

As r increases to the limiting case of two interacting rings, we observe maxima in $P_{\rm vdW}$, at which point the decay rate of $E_{\rm vdW}$ is minimized. In this case, $P_{\rm vdW}^{\rm ring-ring}(R,D) = -5 - 5/[1+4(R/D)^2] + 4[1 + 2(R/D)^2]/[1+4(R/D)^2+6(R/D)^4]$, from which one sees that $P_{\rm vdW}^{\rm ring-ring} \to -5$ in the short range as $R/D \to \infty$ and the interaction between these two rings (or 1-spheres) mimics that of two parallel, infinitely long wires (see Fig. 2). At intermediate distances, maxima occur at $D/R = 1.33$ and are bound above by $P_{\rm vdW} = -4.88$. The fact that $P_{\rm vdW}^{\rm ring-ring}$ is equivalent to that of a point particle, A, located directly above the perimeter (not the centroid) of a ring illustrates that these maxima result from a competition between the vdW interactions of A with adjacent and distant sectors of the ring.

To investigate the vdW scaling behavior in porous 2D materials, we now consider a model system consisting of periodic layers tiled by hexagons with inner and outer radii, $\overline{r}$ and $\overline{R}$ (denoted by layer$[\overline{r}, \overline{R}]$). When interacting with a point particle, A, numerical evaluation [55] of $E_{\rm vdW}$ shows that $P_{\rm vdW}^{\rm A-layer} \to 0$ in the short range once pores are present in the periodic layer, and approaches D^{-4} (as expected for A interacting with an infinite non-porous 2D surface [50, 51]) for $D \gtrsim 20$ Å in the layer$[10, 10]$ case. This short-range behavior is completely analogous to $P_{\rm vdW}^{\rm A-ann}$, which again highlights the difference between porous and non-porous molecules and materials. Numerical results for $P_{\rm vdW}$ in stacked bilayers

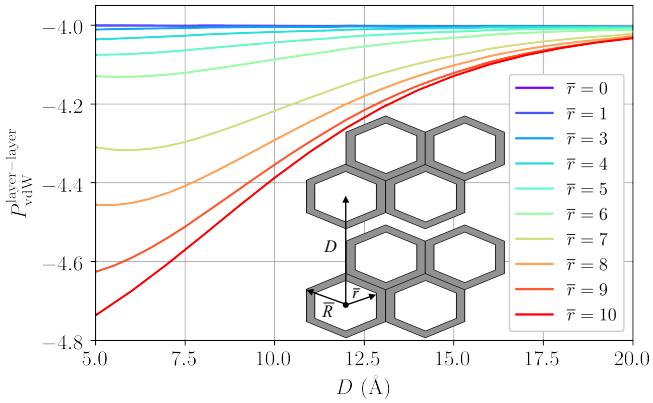

FIG. 3. Effective power law exponents, $P_{\rm vdW}^{\rm layer-layer}$, for the pairwise vdW interaction between two stacked periodic hexagonal layers with $\overline{R} = 10$ as a function of $\overline{r}$ and D (all in Å). When $\overline{r} \neq 0$, such porous 2D materials exhibit fundamentally different behavior (including the formation of minima in $P_{\rm vdW}$) than the limiting case of two infinite non-porous plates ($\overline{r} = 0$), which has $P_{\rm vdW} = -4$ for all interlayer separations.

with $\overline{R} = 10$ Å are depicted in Fig. 3, where one again sees that the mere presence of a pore leads to remarkably different vdW scaling behavior. As expected for the pairwise vdW interaction between two infinite non-porous plates, $P_{\rm vdW} = -4$ for all D when $\overline{r} = 0$. In porous 2D materials, however, $P_{\rm vdW}$ strongly depends on $\overline{r}/\overline{R}$, with larger values leading to slower convergence to this asymptotic limit. In fact, one can even observe minima in $P_{\rm vdW}$ for $\overline{r}/\overline{R}$ values between 0.5 (at $D \approx 0.65\,\overline{R}$) and 1.0 (at $D \approx 0.20\,\overline{R}$), at which point the decay rate of $E_{\rm vdW}$ is maximized. In contrast to porous macrocycles, porous bilayer materials *always* have a faster decay rate than their non-porous analogs, and therefore approach asymptotic behavior from below. Not surprisingly, $P_{\rm vdW}$ is also a function of the hexagonal ring size, with larger values of $\overline{R}$ extending the range of non-asymptotic behavior to $D \gtrsim 100$ Å (*e.g.*, for $\overline{R} = 40$ Å) [55].

To explore how well these models describe the vdW scaling in real porous 2D molecules and materials, we now focus on macrocycle dimers (MC) and periodic bilayers (BL) of three popular COF systems [6–8, 48, 60, 61]: COF-5, TP-COF, and HHTP-DPB COF (Fig. 4, top panel). To do so, we compare $P_{\rm vdW}$ from the analytical ann$[r, R]$ and numerical layer$[\overline{r}, \overline{R}]$ models introduced herein with dispersion-inclusive density functional theory (*i.e.*, PBE [62] in conjunction with the effective pairwise TS-vdW approach [63, 64]) in Quantum ESPRESSO [55, 65]. With a range of simple atom-to-atom distance estimates for the inner and outer COF radii, these models provide $P_{\rm vdW}$ values in remarkable agreement with PBE+TS-vdW (Fig. 4, bottom panel). Further optimization of these parameters leads to physical values for r/R ($\overline{r}/\overline{R}$) of 0.72 (0.88), 0.75 (0.88), and 0.81 (0.93), for COF-5, TP-COF, and HHTP-DPB COF, respectively; these values are essentially contained in the ranges estimated above and yield even better agreement between the curves [55]. Interestingly, these values are in the neighborhood of $r/R = 0.75$, which corresponds to the stationary point of inflection in $P_{\rm vdW}^{\rm ann-ann}$; as such, COF macrocycle dimers have $P_{\rm vdW}$ which ex-

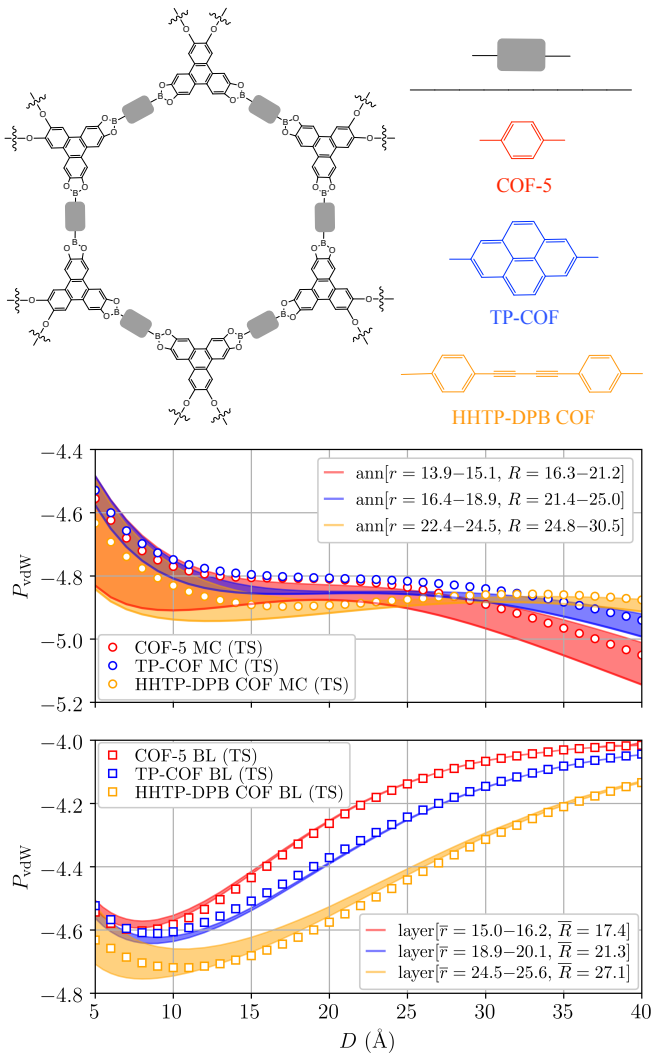

FIG. 4. *Top.* 2D building blocks for COF-5 (red), TP-COF (blue), and HHTP-DPB COF (orange). In this work, COF macrocycles have capped terminal hydroxyl (−OH) groups. *Bottom.* Effective power law exponents for stacked COF macrocycle dimers (MC) and periodic bilayers (BL) obtained using the analytical ann$[r, R]$ and numerical layer$[\overline{r}, \overline{R}]$ models introduced in this work (solid lines), and the effective pairwise PBE+TS-vdW approach (TS, circles and squares). $P_{\rm vdW}^{\rm ann-ann}$ ($P_{\rm vdW}^{\rm layer-layer}$) are provided for a range of r and R ($\overline{r}$ and $\overline{R}$) based on simple estimates of the radii in these systems [55], and are in high fidelity with the first-principles based PBE+TS-vdW approach. Quite interestingly, we find that these COF systems have relative pore sizes that lead to characteristic features such as extended plateaus (MC) and minima (BL) in $P_{\rm vdW}$.

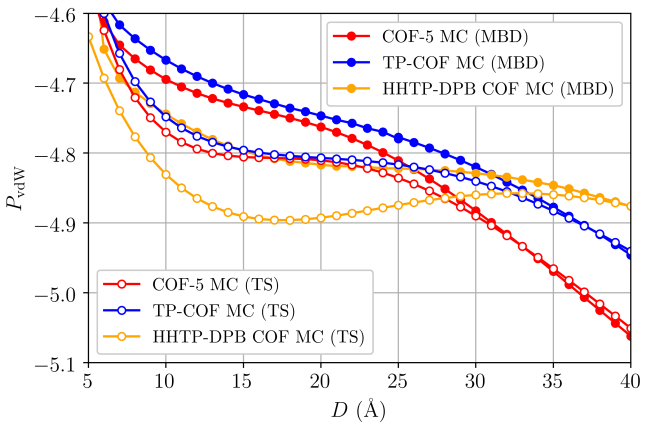

FIG. 5. Effective power law exponents for stacked COF macrocycle dimers (MC) at the effective pairwise (TS, open circles) and many-body dispersion (MBD, closed circles) levels.

hibit extended plateaus across the quite relevant range of $D \approx 10{-}40$ Å. For the COF bilayers, we also find characteristic minima in P_{vdW} at $D \approx 7{-}10$ Å, where the decay rate of E_{vdW} has peaked.

In analogy to the ACFDT-RPA treatment of the $A-$ann model system above, we employed the many-body dispersion (MBD) model [66–70] in conjunction with PBE to investigate how higher-order vdW interactions might influence the scaling behavior in the COF macrocycle dimers. As depicted in Fig. 5, we find that these relatively short-ranged and anisotropic interactions lead to some deviations in P_{vdW} at small/intermediate distances and converge to pairwise behavior for $D \gtrsim 30{-}35$ Å. Of greater interest is the fact that the extended plateaus in P_{vdW} are a robust feature of the vdW scaling landscape, with many-body effects actually enhancing P_{vdW} for $D = 1{-}3$ nm, a range of distances quite relevant to COF self-assembly [48, 49].

These unique power laws—which originate from the void space present in porous 2D molecules and materials—provide insight into the self-assembly and design of complex nanostructures. For stacked macrocycle dimers, extended plateaus and maxima in P_{vdW} demonstrate that a range of relative pore sizes lead to a nontrivial interplay between P_{vdW}, which favors small (large) pores in the short (long) range, and E_{vdW}/atom, which favors small pores for all intermonomer separations. In extended systems, however, P_{vdW} and E_{vdW}/atom work in tandem across all interlayer distances, and can collectively bias the number of layers preferred in a 2D material. Since the onset and extent of these effects are governed by r and R (or $\overline{r}$ and $\overline{R}$), these quantities can be leveraged to influence the self-assembly of porous nanostructures ranging from stacked macrocycles to complex multi-layered COF architectures.

All authors acknowledge Greg Ezra, Jan Hermann, Hsin-Yu Ko, and Alexandre Tkatchenko for critically reading the manuscript. This work was partially supported by start-up funding from Cornell University and the Cornell Center for Materials Research (CCMR) with funding from the National Science Foundation MRSEC program (DMR-1719875). This research used resources of the National Energy Research Scientific Computing Center, which is supported by the Office of Science of the U.S. Department of Energy under Contract No. DE-AC02-05CH11231.

REFERENCES

[1] K. S. Novoselov, D. Jiang, F. Schedin, T. J. Booth, V. V. Khotkevich, S. V. Morozov, and A. K. Geim, Proc. Natl. Acad. Sci. U.S.A. **102**, 10451 (2005).
[2] K. S. Novoselov, S. V. Morozov, T. M. G. Mohinddin, L. A. Ponomarenko, D. C. Elias, R. Yang, I. I. Barbolina, P. Blake, T. J. Booth, D. Jiang, J. Giesbers, E. W. Hill, and A. K. Geim, Phys. Status Solidi B **244**, 4106 (2007).
[3] C. Zhi, Y. Bando, C. Tang, H. Kuwahara, and D. Golberg, Adv. Mater. **21**, 2889 (2009).
[4] A. A. Balandin, Nat. Mater. **10**, 569 (2011).
[5] R. Mas-Ballesté, C. Gómez-Navarro, J. Gómez-Herrero, and F. Zamora, Nanoscale **3**, 20 (2011).
[6] A. P. Côté, A. I. Benin, N. W. Ockwig, M. O'Keeffe, A. J. Matzger, and O. M. Yaghi, Science **310**, 1166 (2005).
[7] A. P. Côté, H. M. El-Kaderi, H. Furukawa, J. R. Hunt, and O. M. Yaghi, J. Am. Chem. Soc. **129**, 12914 (2007).
[8] E. L. Spitler and W. R. Dichtel, Nat. Chem. **2**, 672 (2010).
[9] A. Nagai, Z. Guo, X. Feng, S. Jin, X. Chen, X. Din, and D. Jiang, Nat. Commun. **2**, 536 (2011).
[10] X. X. Feng, X. Ding, and D. Jiang, Chem. Soc. Rev. **41**, 6010 (2012).
[11] S. Ding and W. Wang, Chem. Soc. Rev. **42**, 548 (2013).
[12] C. S. Diercks and O. M. Yaghi, Science **355**, eaal1585 (2017).
[13] H. Li, M. Eddaoudi, M. O'Keeffe, and O. M. Yaghi, Nature **402**, 276 (1999).
[14] S. L. James, Chem. Soc. Rev. **32**, 276 (2003).
[15] D. Wu, F. Xu, B. Sun, R. Fu, H. He, and K. Matyjaszewski, Chem. Rev. **112**, 3959 (2012).
[16] S. Kitagawa, R. Kitaura, and S. Noro, Angew. Chem. Int. Ed. **43**, 2334 (2004).
[17] S. Wan, J. Guo, J. Kim, H. Ihee, and D. Jiang, Angew. Chem. Int. Ed. **48**, 5439 (2009).
[18] H. Song, J. J. Wu, H. Cheng, and F. Kang, Joule **2**, 442 (2018).
[19] T. Liu, J. Ding, Z. Su, and G. Wei, Mater. Today Energy **6**, 79 (2017).
[20] R. W. Tilford, S. J. Mugavero, P. J. Pellechia, and J. J. Lavigne, Adv. Mater. **20**, 2741 (2008).
[21] J. Lee, O. K. Farha, J. Roberts, K. A. Scheidt, S. T. Nguyen, and J. T. Hupp, Chem. Soc. Rev. **38**, 1450 (2009).
[22] M. Vallet-Regí, F. Balas, and D. Arcos, Angew. Chem. Int. Ed. **46**, 7548 (2007).
[23] D. Chimene, D. L. Alge, and A. K. Gaharwar, Adv. Mater. **27**, 7261 (2015).
[24] S. Xie, L. Tu, Y. Han, L. Huang, K. Kang, K. U. Lao, P. Poddar, C. Park, D. A. Muller, R. A. DiStasio Jr.,

and J. Park, Science **359**, 1131 (2018).
[25] L. A. Ponomarenko, A. K. Geim, A. A. Zhukov, R. Jalil, S. V. Morozov, K. S. Novoselov, I. V. Grigorieva, E. H. Hill, V. V. Cheianov, V. I. Fal'Ko, K. Watanabe, T. Taniguchi, and R. V. Gorbachev, Nat. Phys. **7**, 958 (2011).
[26] S. J. Haigh, A. Gholinia, R. Jalil, S. Romani, L. Britnell, D. C. Elias, K. S. Novoselov, L. A. Ponomarenko, A. K. Geim, and R. Gorbachev, Nat. Mater. **11**, 764 (2012).
[27] A. K. Geim and I. V. Grigorieva, Nature **499**, 419 (2013).
[28] K. S. Novoselov, A. Mishchenko, A. Carvalho, and A. H. C. Neto, Science **353**, aac9439 (2016).
[29] D. Langbein, *Theory of van der Waals Attraction* (Springer, Berlin, 1974).
[30] V. A. Parsegian, *van der Waals Forces: A Handbook for Biologists, Chemists, Engineers, and Physicists* (Cambridge University Press, Cambridge, 2005).
[31] I. G. Kaplan, *Intermolecular Interactions: Physical Picture, Computational Methods and Model Potentials* (Wiley, New York, 2006).
[32] A. J. Stone, *The Theory of Intermolecular Forces*, 2nd ed. (Oxford University Press, Oxford, 2013).
[33] J. L. Beeby, J. Phys. C: Solid State Phys. **4**, L359 (1971).
[34] P. Loskill, H. Hähl, T. Faidt, S. Grandthyll, F. Müller, and K. Jacobs, Adv. Colloid Interface Sci. **179**, 107 (2012).
[35] P. Loskill, J. Puthoff, M. Wilkinson, K. Mecke, K. Jacobs, and K. Autumn, J. R. Soc. Interface **10**, 20120587 (2013).
[36] V. V. Gobre and A. Tkatchenko, Nat. Comm. **4**, 2341 (2013).
[37] A. Ambrosetti, N. Ferri, R. A. DiStasio Jr., and A. Tkatchenko, Science **351**, 1171 (2016).
[38] T. Gould, K. Simpkins, and J. F. Dobson, Phys. Rev. B **77**, 165134 (2008).
[39] L. Spanu, S. Sorella, and G. Galli, Phys. Rev. Lett. **103**, 196401 (2009).
[40] Y. J. Dappe, J. Ortega, and F. Flores, Phys. Rev. B **79**, 165409 (2009).
[41] S. Lebègue, J. Harl, T. Gould, J. G. Ángyán, G. Kresse, and J. F. Dobson, Phys. Rev. Lett. **105**, 196401 (2010).
[42] A. J. Misquitta, J. Spencer, A. J. Stone, and A. Alavi, Phys. Rev. B **82**, 075312 (2010).
[43] A. J. Misquitta, R. Maezono, N. D. Drummond, A. J. Stone, and R. J. Needs, Phys. Rev. B **89**, 045140 (2014).
[44] K. A. Makhnovets and A. K. Kolezhuk, Phys. Rev. B **96**, 125427 (2017).
[45] P. S. Venkataram, J. Hermann, A. Tkatchenko, and A. W. Rodriguez, Phys. Rev. Lett. **118**, 266802 (2017).
[46] J. F. Dobson, A. White, and A. Rubio, Phys. Rev. Lett. **96**, 073201 (2006).
[47] T. Gould, E. Gray, and J. F. Dobson, Phys. Rev. B **79**, 113402 (2009).
[48] A. D. Chavez, B. J. Smith, M. K. Smith, P. A. Beaucage, B. H. Northrop, and W. R. Dichtel, Chem. Mater. **28**, 4884 (2016).
[49] D. N. Bunck and W. R. Dichtel, J. Am. Chem. Soc. **135**, 14952 (2013).
[50] A. M. C. Reyes and C. Eberlein, Phys. Rev. A **80**, 032901 (2009).
[51] A. Ambrosetti, P. L. Silvestrelli, and A. Tkatchenko, Phys. Rev. B **95**, 235417 (2017).
[52] H. Kim, J. O. Sofo, D. Velegol, M. W. Cole, and A. A. Lucas, Langmuir **23**, 1735 (2007).
[53] J. F. Dobson, T. Gould, and G. Vignale, Phys. Rev. X **4**, 021040 (2014).
[54] C. A. S. Batista, R. G. Larson, and N. A. Kotov, Science **350**, 1242477 (2015).
[55] See Supplemental Material at [URL will be inserted by publisher] for more details.
[56] D. Bohm and D. Pines, Phys. Rev. **92**, 609 (1953).
[57] M. Gell-Mann and K. A. Brueckner, Phys. Rev. **106**, 364 (1957).
[58] O. Gunnarsson and B. I. Lundqvist, Phys. Rev. B **13**, 4274 (1976).
[59] D. C. Langreth and J. P. Perdew, Phys. Rev. B **15**, 2884 (1977).
[60] S. Wan, J. Guo, J. Kim, H. Ihee, and D. Jiang, Angew. Chem. Int. Ed. **120**, 8958 (2008).
[61] E. L. Spitler, B. T. Koo, J. L. Novotney, J. W. Colson, F. J. Uribe-Romo, G. D. Gutierrez, P. Clancy, and W. R. Dichtel, J. Am. Chem. Soc. **133**, 19416 (2011).
[62] J. P. Perdew, K. Burke, and M. Ernzerhof, Phys. Rev. Lett. **77**, 3865 (1996).
[63] A. Tkatchenko and M. Scheffler, Phys. Rev. Lett. **102**, 073005 (2009).
[64] N. Ferri, R. A. DiStasio Jr., A. Ambrosetti, R. Car, and A. Tkatchenko, Phys. Rev. Lett. **114**, 176802 (2015).
[65] P. Giannozzi *et al.*, J. Phys.: Condens. Matter **29**, 465901 (2017).
[66] A. Tkatchenko, R. A. DiStasio Jr., R. Car, and M. Scheffler, Phys. Rev. Lett. **108**, 236402 (2012).
[67] R. A. DiStasio Jr., O. A. von Lilienfeld, and A. Tkatchenko, Proc. Natl. Acad. Sci. U.S.A. **109**, 14791 (2012).
[68] R. A. DiStasio Jr., V. V. Gobre, and A. Tkatcheno, J. Phys.: Condens. Matter **26**, 213202 (2014).
[69] A. Ambrosetti, A. M. Reilly, R. A. DiStasio Jr., and A. Tkatchenko, J. Chem. Phys. **140**, 18A508 (2014).
[70] M. A. Blood-Forsythe, T. Markovich, R. A. DiStasio Jr., R. Car, and A. Aspuru-Guzik, Chem. Sci. **7**, 1712 (2016).